A TECHNIQUE FOR MEASURING THE DISPLACEMENT VECTOR THROUGHOUT THE BODY OF A PAVEMENT STRUCTURE SUBJECTED TO CYCLIC LOADING

by

William M. Moore
Associate Research Engineer

and

Gilbert Swift
Research Instrumentation Engineer

Research Report No. 136-2
Design and Evaluation of Flexible Pavements
Research Study 2-8-69-136

Sponsored by

The Texas Highway Department
In Cooperation with the
U. S. Department of Transportation
Federal Highway Administration

August, 1971

TEXAS TRANSPORTATION INSTITUTE
Texas A&M University
College Station, Texas

PREFACE

This is the second report issued under Research Study 2-8-69-136, Design and Evaluation of Flexible Pavements, being conducted at the Texas Transportation Institute as part of the cooperative research program with the Texas Highway Department and the Department of Transportation, Federal Highway Administration.

The first report is

> "Seasonal Variations of Pavement Deflections in Texas," by Rudell Poehl and Frank H. Scrivner, Research Report 136-1, Texas Transportation Institute, January, 1971.

The authors wish to thank all members of the Institute who assisted in this research. They would like to express special appreciation to Mr. Frank H. Scrivner and Mr. Lionel J. Milberger. Their help throughout the study has been particularly valuable. Thanks are also due Mr. C. H. Michalak for his assistance in the data reduction phase and Mr. John Salyer for his assistance during the fabrication and testing phases.

The authors are grateful to the Texas Highway Department for their interest and cooperation. They would like to express special gratitude to Messrs. James L. Brown and Larry J. Buttler of the Highway Design Division for their assistance and support of this research and to the personnel of Districts 8 and 17 for their assistance during the development of the drilling technique.

ABSTRACT

A measuring technique was developed to determine the displacement vector throughout the body of a pavement structure subjected to Dynaflect loading. The instrumentation used for these measurements is described and the displacement vector fields observed in three different pavement structures are shown and compared.

Key Words: Deflections, Displacement, Measurement, Pavement-Structure, Vector-Field.

SUMMARY

A technique is described for observation of the displacement vector field, or motions of the points within the body of a pavement structure under the influence of cyclic loading. An oscillating load of 1000 lbs. at 8 cycles per second produced by the Dynaflect is applied to the surface. The vertical and horizontal components of the displacements were measured by emplacing a sensor in a small hole drilled into the body of the pavement. Observed displacements are shown for three different pavement structures. The measurements were repeated at a different location on each structure and the replicate data sets are shown and compared. Their differences are seen to be small in comparison with the differences observed between structures.

The measured displacement fields are shown to have considerable similarity to fields computed for layered elastic structures. It is concluded that a practical fieldworthy technique has been developed for observing the vector displacement response of a pavement structure and that the development of a useful and practical mathematical model representing the displacement vector throughout a pavement structure should be possible.

IMPLEMENTATION STATEMENT

The end results of this research study are expected to provide a significant improvement to the empirical deflection equation currently being used in the Texas Highway Department's flexible pavement design system. Use of the present equation has pointed out several weak points and a pressing need for a more accurate one. This report describes the measurement technique developed and typical data to be used to improve the equation.

TABLE OF CONTENTS

LIST OF FIGURES

1. INTRODUCTION

This is a progress report on Phase 2 of a research study entitled "Design and Evaluation of Flexible Pavements" being conducted by the Texas Transportation Institute and sponsored by the Texas Highway Department and the Federal Highway Administration. The objective of this phase of the research, as quoted from the Study Proposal, is "to develop from full-scale testing, a mathematical model estimating the displacement vector at any given point within a pavement structure subjected to Dynaflect loading, given this vector at the surface, the thickness of each layer and a stiffness parameter for each material." Two different models for estimating the vertical component of the displacement vector on a pavement's surface were developed in Research Study 32 (1, 2). The second and more accurate model was used in the development of the flexible pavement design system (3) which is being expanded and implemented in study 123 (4). Use of this model has pointed out several weak points and a pressing need for a still more accurate one.

An accurate model for predicting the displacement vector within any given pavement structure will provide design engineers with a means of calculating strains within the structure and will be an important step in the development of a more realistic approach to pavement design. Thus, it is expected that this study will represent a significant step toward obtaining a more rational pavement design theory.

Several researchers have reported measurements of stresses and strains in situ (5, 6, 7, 8). However, placing stress or strain sensors within a pavement structure tends to destroy the continuity of the material and therefore alters the distribution of the quantities being measured. In contrast, displacement measurements should be substantially unaffected by small perturbations of the system.

Any displacement measurement requires a reference point. As pointed out in Reference 9, the Dynaflect* technique of applying a cyclic force makes it possible to employ an inertial reference point which is immune to measurement errors caused by reference point motion. Other methods of measuring displacement require a physical, tangible, reference point which must be sufficiently remote to remain undisturbed during the measurement, at least to the extent set by the desired accuracy of the measurement. Such a point would be quite deep or quite far away if on the surface. Thus, the measurement would require the determination of an extremely small change in a relatively large distance, a requirement which is believed to lead to unacceptably large errors. Accordingly an extention of the Dynaflect measuring technique, employing geophones as displacement sensors, was adopted for this study.

Surface deflections of a pavement structure, as normally measured with the Dynaflect, provide insufficient data to define the response of the entire structure to the loading on its surface. Thus, measurement of the displacement vector field throughout the pavement structure was undertaken in this study to provide data for developing the model

* Registered trademark, Radiation Engineering & Manufacturing Company (REMCO), 7450 Winscott Road, Fort Worth, Texas.

required in the study's objective, or for verifying existing models such as linear elasticity, linear viscoelasticity, etc.

The purpose of this report is to describe the apparatus and technique developed to measure both horizontal and vertical components of the displacement vector. It includes typical measurements obtained, as well as the replication errors encountered.

2. SCOPE OF MEASUREMENTS PROGRAM

The A&M pavement test facility is being used to obtain data for analysis. This facility, located at the University's Research Annex, was constructed for the purpose of providing a means for evaluating nondestructive testing techniques, and more particularly, for evaluating testing equipment purporting to furnish information concerning the in situ characteristics of the individual layers in a flexible pavement. It consists of thirty-two 12 x 40 ft. test sections having different structural characteristics in accordance with the principles of statistical experiment design. The design of the facility is described in detail in Reference 1. Plan and cross-sectional views of the test facility are shown in Figure 1.

The displacement vector field of a test section is induced by loading the section with a Dynaflect. This instrument, shown in Figure 2, produces a vertical dynamic load of 1000 pounds, oscillating sinusoidally with time at 8 Hz (cycles per second), which is applied to the surface through two steel wheels spaced 20 inches apart. A complete description is given in References 9 and 10. Vertical displacement measurements are made on the surface of the pavement using low-frequency geophones whose output voltage is directly proportional to the amplitude of the sinusoidal motion.

The displacement vector field was determined on a test section by measuring separately the horizontal and vertical components of motion at selected depths and horizontal distances from the points of application of the surface loads. To make an individual component measurement a miniature geophone -- either one designed for horizontal motion or one

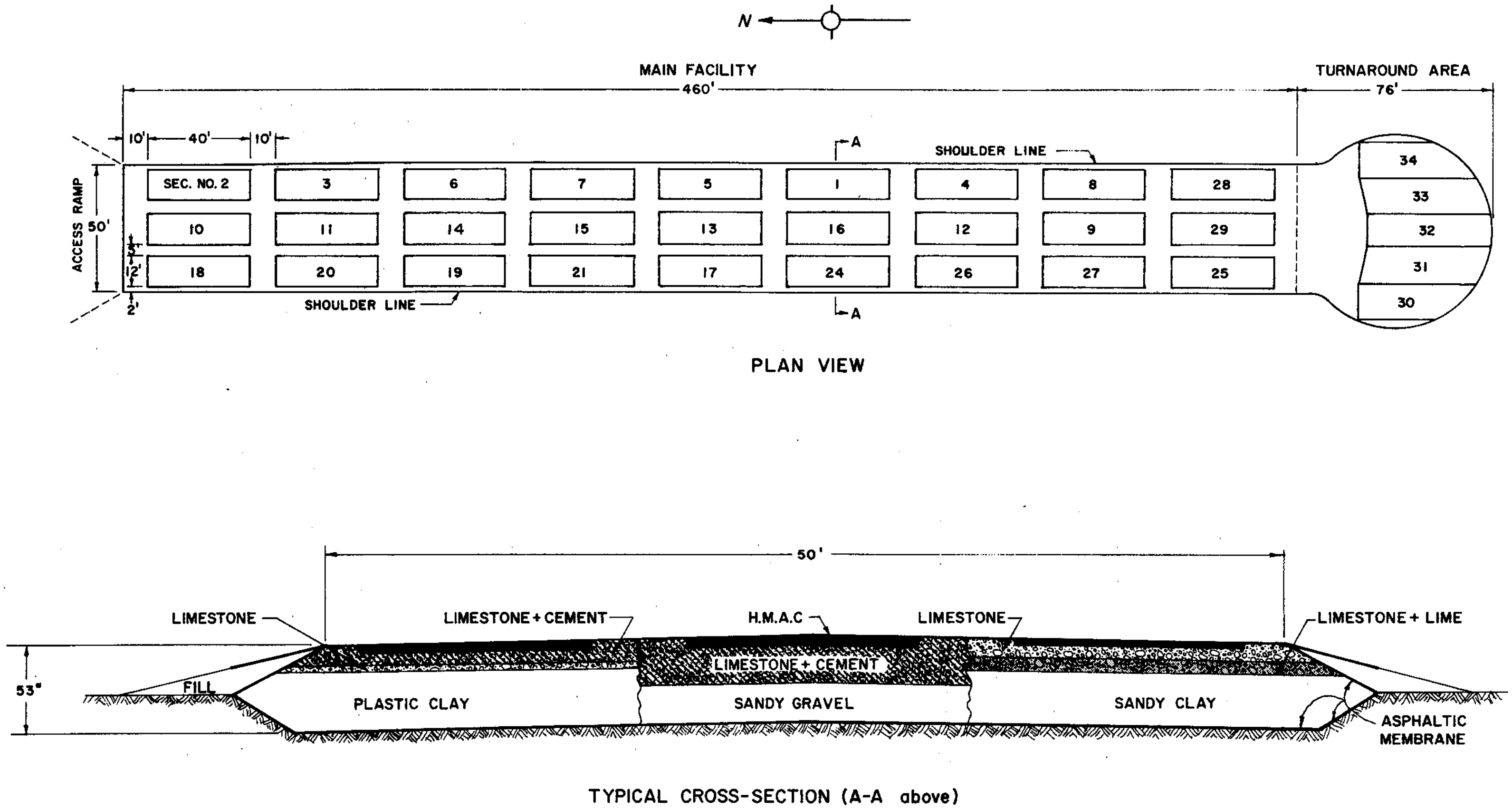

Figure 1: Texas A&M pavement test facility.

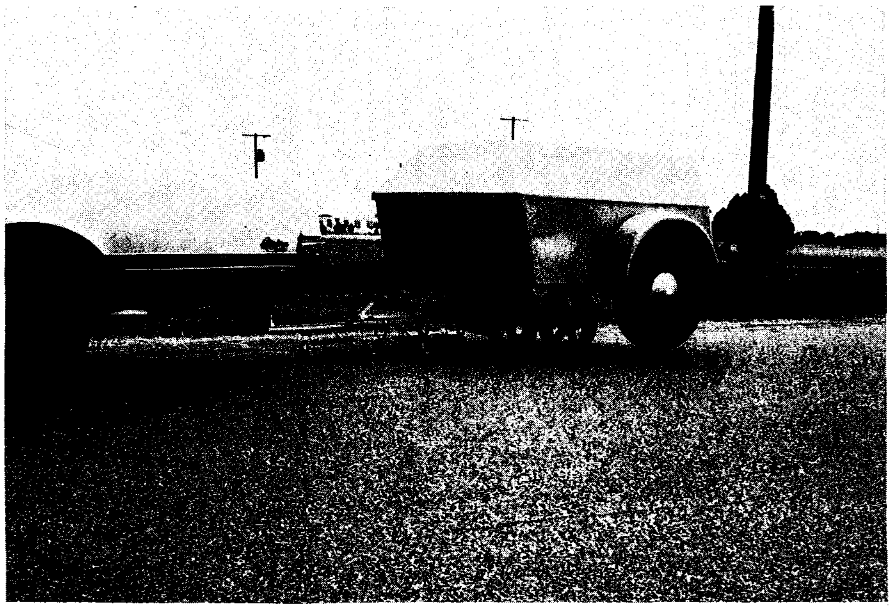

Figure 2: Dynaflect trailer in normal use with five-geophone array on pavement surface.

designed for vertical motion -- was clamped in place in a small diameter hole drilled vertically in the pavement section. The measurement depth was altered by clamping the geophone at various depths, while the horizontal distance from the points of application of the surface load was altered by moving the Dynaflect forward on the surface various distances. Utilizing this concept as illustrated in Figure 3, sufficient measurements were made to define both the vertical and horizontal component fields in the region from zero to about 5 feet in depth and from approximately 1 to 18 feet in horizontal distance. Because of the 20 inch spacing of the Dynaflect load wheels, it was not practical to make measurements at horizontal distances less than 10 inches.

To date displacement vector fields have been measured at two locations on each of three test sections. The planned program includes replicate measurements on all thirty-two of the test sections. Replicate measurements, made on opposite ends of each test section, will permit analysis of overall precision. Replication errors observed on a test section reflect not only the variability of the measuring process but also include the effects of variations in the structural properties of the section. The combined variability will define the limiting prediction accuracy for the displacement model being sought.

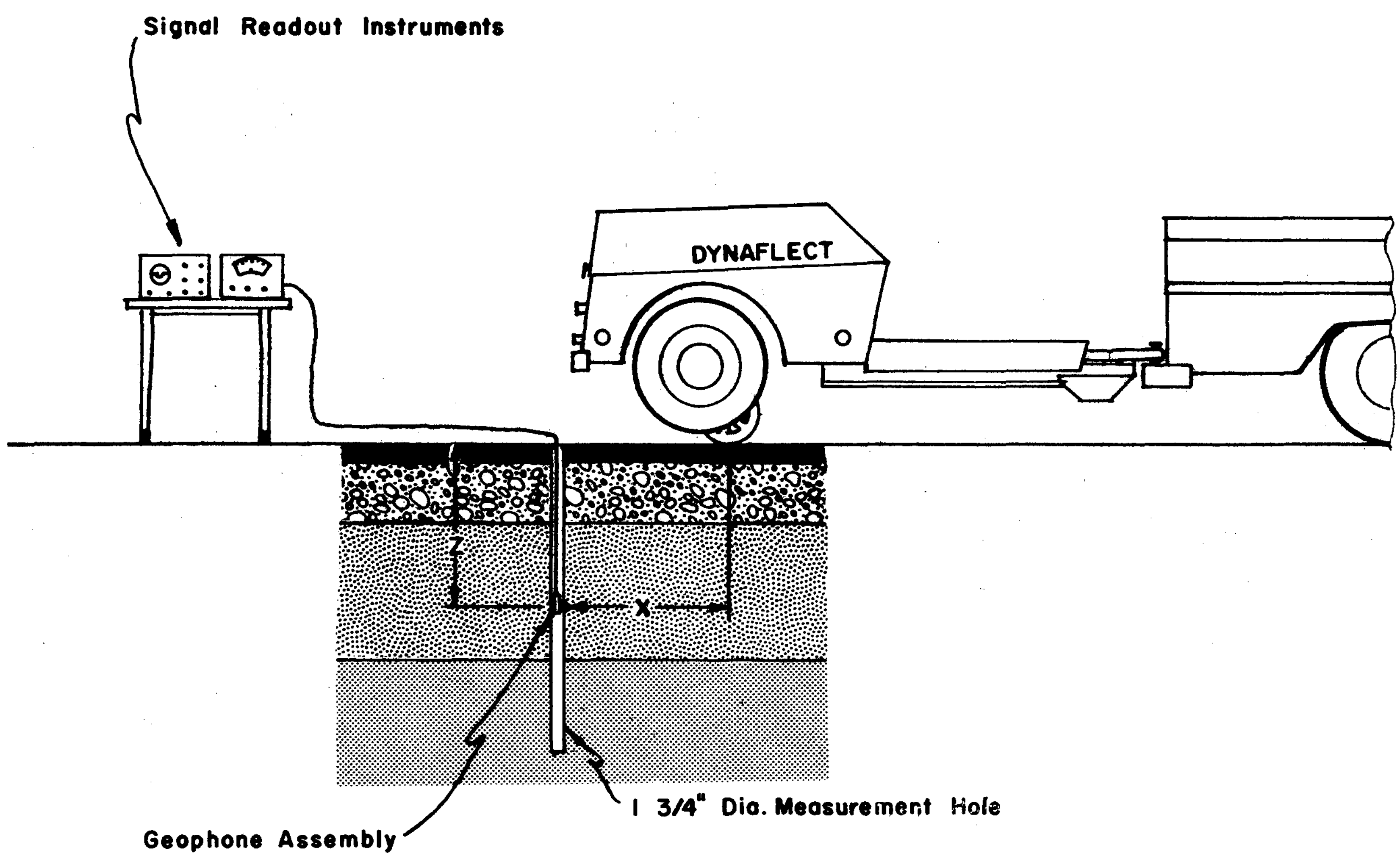

Figure 3: Conceptual representation of the technique used to measure vector displacements within a pavement section.

3. MEASURING TECHNIQUE

3.1 Basic Technique

Extension of the Dynaflect technique to the measurements of the displacement vector throughout the pavement structure was accomplished by using a pair of suitable geophones -- one responsive only to the vertical component of motion, the other responsive only to the horizontal component -- and clamping them one at a time at selected depths in a single hole in the structure. With either geophone placed at a given depth, the Dynaflect was positioned at a succession of locations on the surface ranging from directly above the hole up to 18 feet away.

3.2 Geophone Emplacement

In order to minimize disturbance to the pavement sections, miniature geophones were obtained and an emplaceable assembly was designed which was sufficiently small to fit within a 1-3/4 inch diameter hole. The down-hole geophone assembly is shown in Figure 4. It comprises a waterproof aluminum housing in which one geophone, either horizontal or vertical, is mounted. Two spring-loaded pistons can be released to expand outward and clamp the device in the hole. Flexible steel cables (fishing leader wire) extend above the surface to permit the release and retraction of the pistons. A removable hollow rod, through which the electrical output cable passes, permits the 1-5/8 inch diameter device to be lowered into the hole with the pistons retracted. At the desired depth the pistons are released. The rod is then disconnected and removed from the hole, leaving the unit in place with slack wires extending to the surface. The unit is retrieved by reversing this procedure. A cross section of the down-hole device is shown in Figure 5.

Figure 4: Subsurface geophone assembly being placed in hole in pavement section.

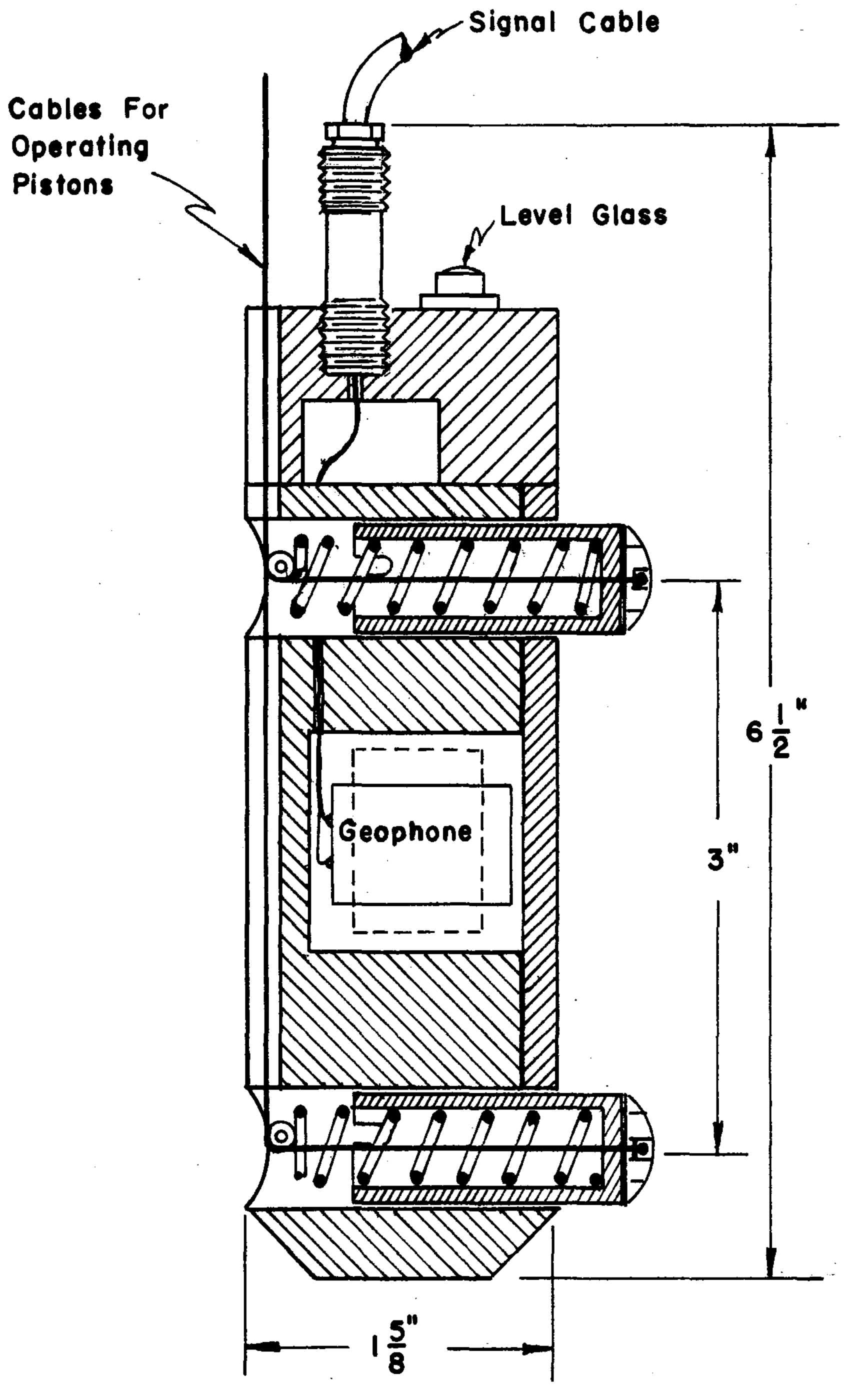

Figure 5: Cross-sectional view of subsurface geophone assembly.

3.3 Drilling Technique

After disappointing results were obtained with several types of drill-rigs and drill-bits, a satisfactory combination was found. All of the successful holes, useable for geophone emplacement, have been drilled with a Clipper Core Drill Model D-30-P using a diamond core-barrel, 1-3/4 diameter by 14 inches long. This drill, shown in Figure 6, is used with a continuous flow of compressed air while penetrating the hot-mix asphaltic concrete surface layer and the limestone base or subbase layers. The same core-barrel is employed, without air-flow, to penetrate the softer embankment and subgrade materials. Where the material is soft clay, the drill is used without rotation.

Several types of drill-bits which were tried in connection with this work are shown in Figure 7. The diamond core-barrel is at the extreme right.

It was decided before undertaking this work that air must be employed during drilling because water would alter or damage the pavement sections. In spite of this precaution, water trapped in the embankment material invaded several of the holes during the measurement period within one or two hours after hole completion. No adverse effects were attributable to this water in those sections in which it was possible to complete the measurement sequence. In one group of sections, however, the hole walls collapsed and prevented emplacement of the geophone. It is planned to drain the excess water from the saturated zones prior to making more measurements on these sections.

3.4 Measuring Procedure

The measuring procedure developed for this investigation began with emplacement of the vertical geophone at the greatest chosen depth.

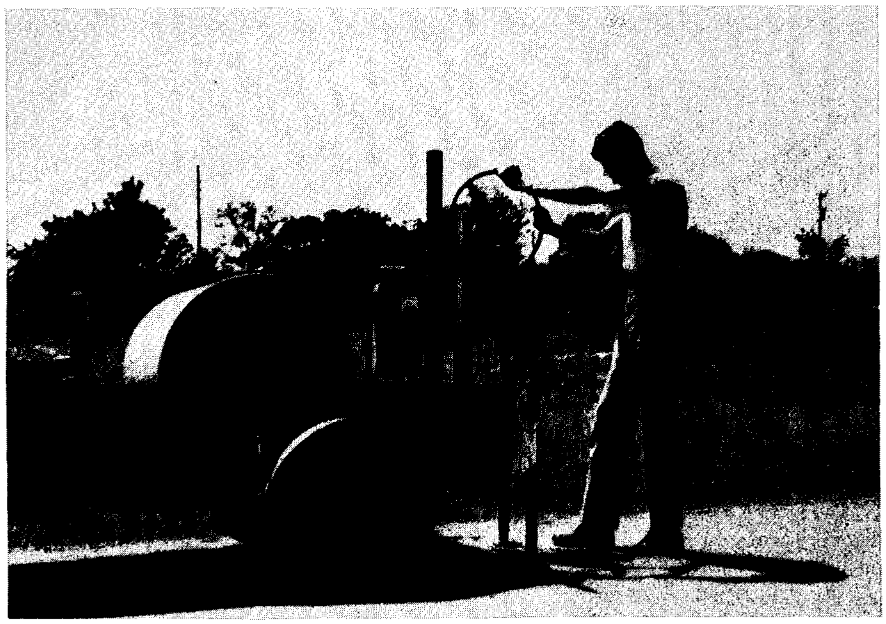

Figure 6: Drill-rig used to bore 1-3/4 inch diameter holes for measurement of displacement vector fields.

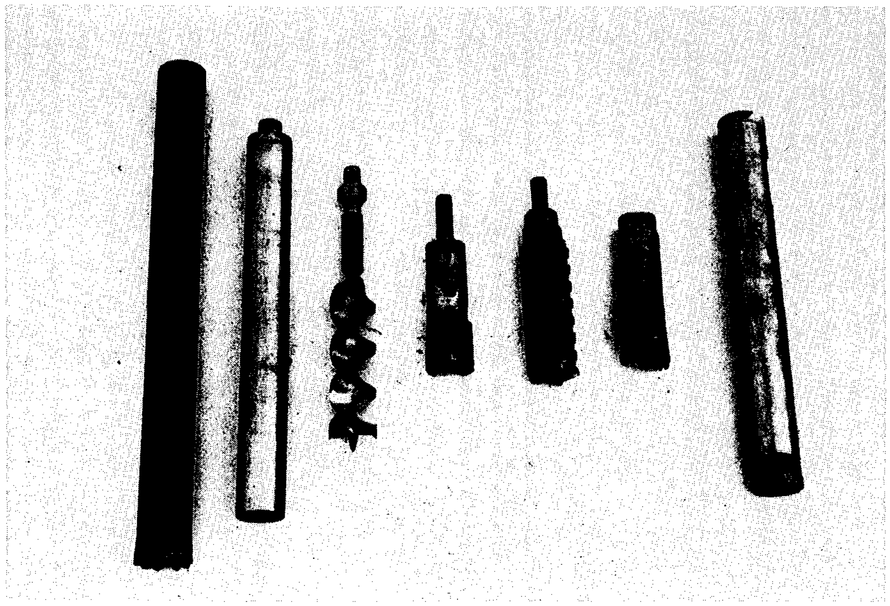

Figure 7: Various drill-bits tried in connection with drilling holes for displacement measurements. Best results were obtained with the diamond core barrel shown at the extreme right.

The Dynaflect was then positioned on the surface directly over the hole. After reading and recording the geophone output voltage the Dynaflect was moved away from the hole to each of a series of preselected distances. The geophone signal was read and recorded at each location. At the end of each such series of measurements the geophone was retrieved and repositioned at a shallower depth in the hole. Upon completion of the entire grid of measurements the above procedure was repeated using the horizontal geophone. When using the latter, in addition to recording the magnitude of its output signal, the phase angle was observed to determine whether the horizontal displacement was toward or away from the load.

Ordinarily one hole and one entire set of vertical and horizontal displacement measurements can be completed within a day. At the end of each set of horizontal or vertical measurements the geophone used for that set was calibrated by observing its response to a 0.005 inch oscillatory motion provided by the Dynaflect calibrator unit. The calibration factor thus established was utilized to convert the recorded voltage readings to displacements in millionths of an inch. Using a Hewlett Packard Model 502A Wave Analyzer to read these voltages, displacements as small as one millionth of an inch could be measured (See Figure 8). Thus far the observed movements have ranged from less than one millionth to two thousandths of an inch.

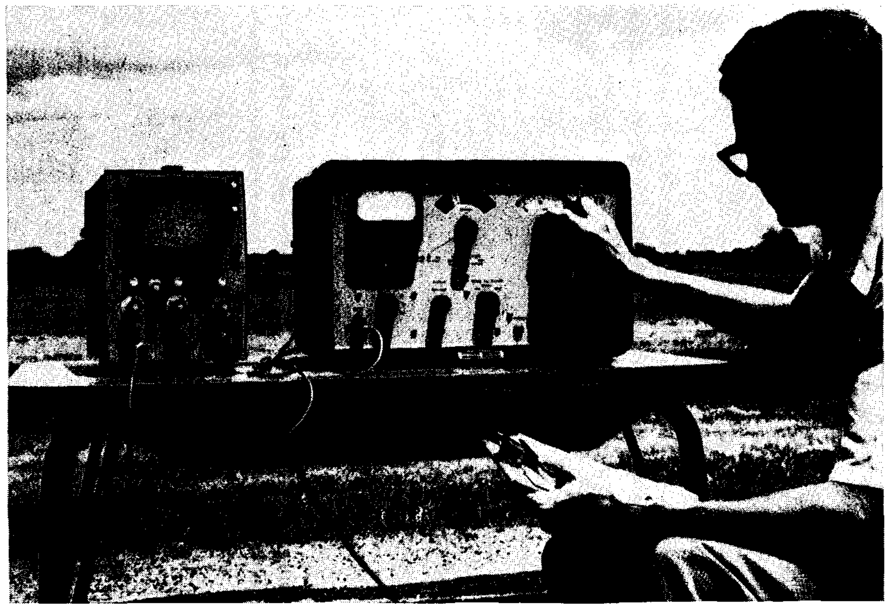

Figure 8: Operator reading the geophone output signal magnitude on Wave Analyzer. The oscilloscope at the left is used to observe the phase angle of the geophone signals to determine direction.

4. <u>Transformation of Measurements to A Single Load Vector Field</u>

As previously mentioned, the dynaflect applies a 1000 lb. load to the surface through two wheels which are spaced 20 inches apart. Hence, when the Dynaflect is centered over a hole, its two load application points are equidistant at a 10 inch radial (horizontal) distance from the hole. Moving the Dynaflect forward a distance, x, along a straight line increases both of these radial distances while maintaining their equality. The radial distance, r, from the hole to either of the load application points is given by

$$r = \sqrt{x^2 + 10^2}.$$

In order to simplify the presentation of the data, the observed measurements were converted to the case of a single 1000 lb. axially symmetrical load acting at a distance, r, from the hole, by assuming that the displacement vectors at any depth, z, produced by the two 500 lb. loads were of equal magnitude and were vectorially additive.

The vertical displacement components produced by each of the two loads are alike in both magnitude and direction; therefore, the vertical component for a single 500 lb. load would be half the measured value, and for a single 1000 lb. load it would be equal to the measured value. This measured value is represented by the symbol, w.

The horizontal components of motion produced by each load wheel are alike in magnitude but, unlike the vertical components, are directed along lines parallel to the radial (horizontal) lines on the surface joining the hole with the individual load application points. Hence, when the Dynaflect is centered over the hole, the horizontal components due to each load wheel are in opposite directions. Since this represents a null of horizontal motion, the horizontal measurement is omitted at this position. The horizontal measurement closest to the loads is made with the Dynaflect axle 6 inches away from the hole and the most remote measurement is made when it is 18 ft. (or 216 inches) away. At any given forward distance, x, (See Figure 9) the horizontal displacement components produced by each load wheel are equal in magnitude but are separated by an angle 2α, where

$$\alpha = \arctan (10/x).$$

Thus the measured horizontal displacement, M_h, is related to the horizontal displacement, u, resulting from a single 1000 lb. load, by

$$u = M_h \sec \alpha$$

as may be verified by reference to Figure 9.

Sec α can be regarded as a correction factor which is applied to the measured values of horizontal displacement to transform them to values which would have been obtained in the assumed axially symmetrical case. Figure 10 is a plot of sec α versus x. From this plot it can be seen that the correction factor approaches unity very quickly as the Dynaflect is moved forward to increase the horizontal distance x. Thus, the principle of Saint-Venant is illustrated, in that the correction factor becomes insignificant at values of x exceeding two or three times the 20-inch distance between the load wheels (11).

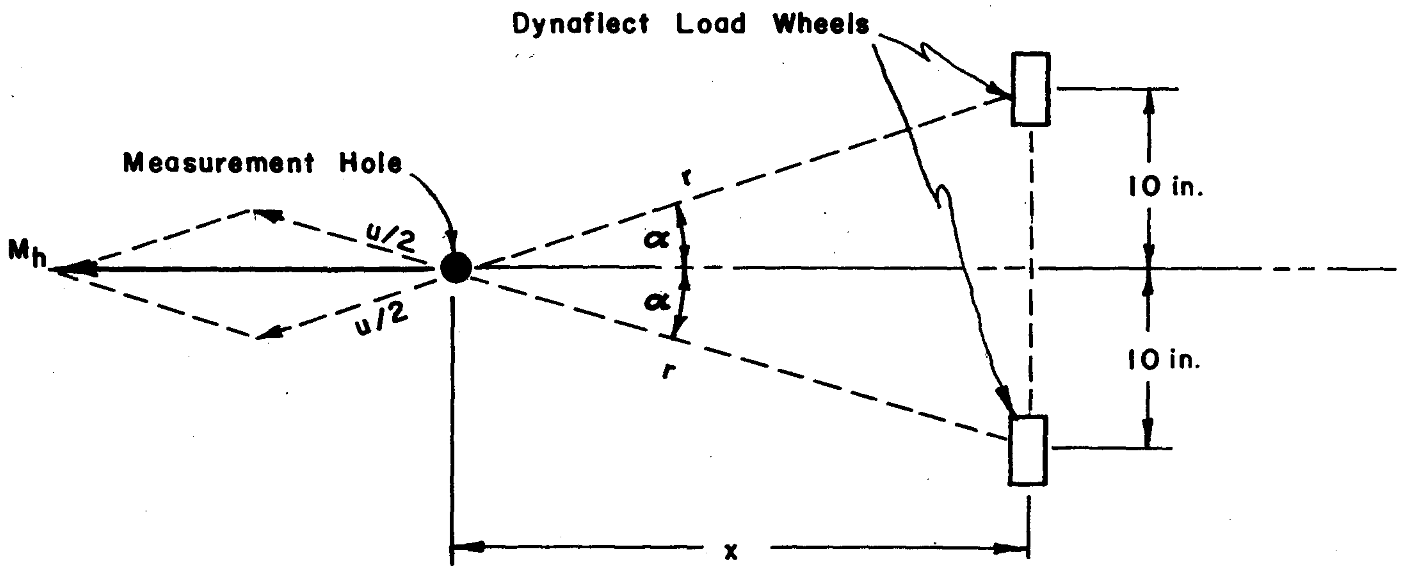

Figure 9: The relation of the horizontal displacement vectors produced by each load wheel to the measured horizontal displacement.

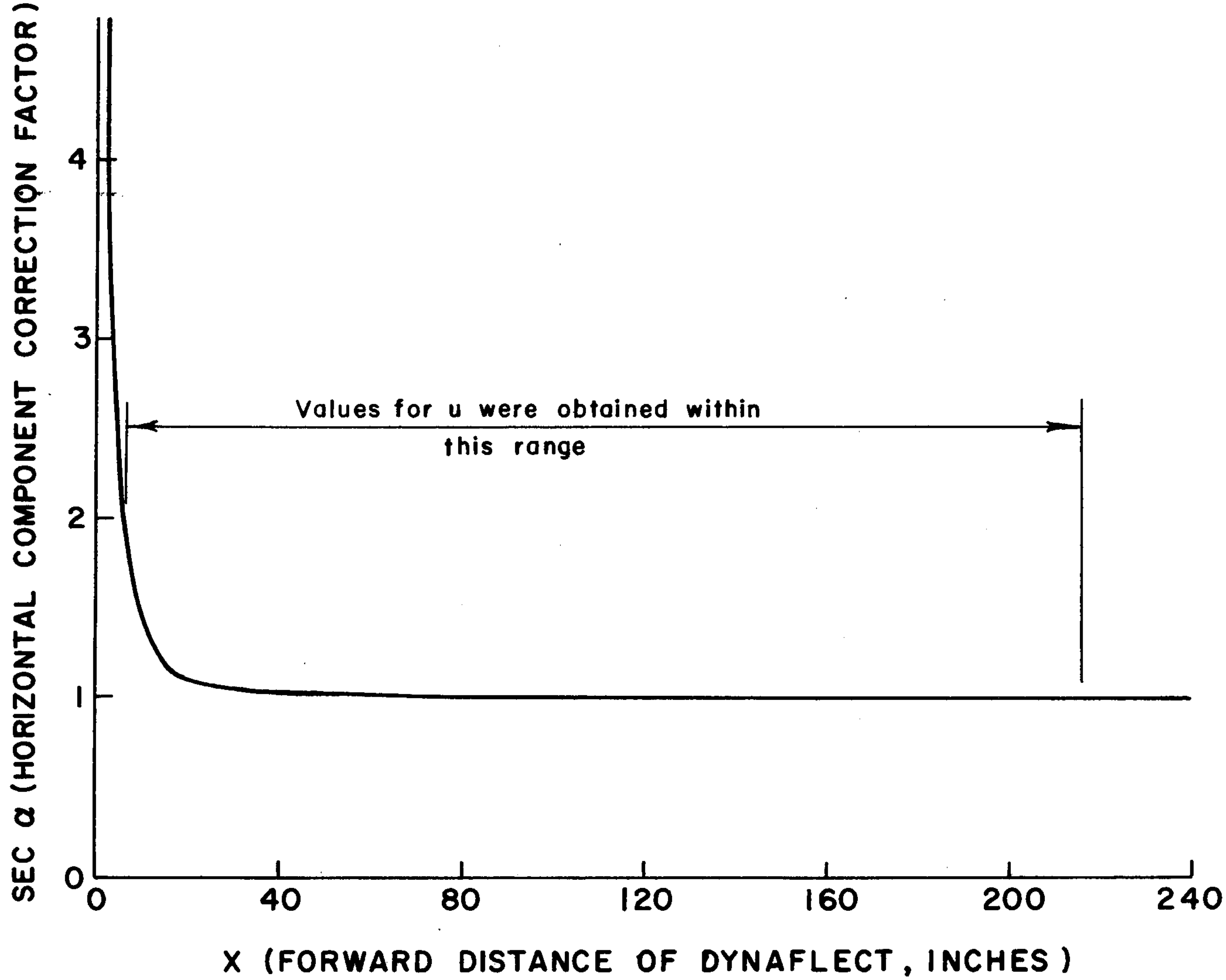

Figure 10: The relationship of forward distance of Dynaflect to the correction factor applied to the measured horizontal displacement in the transformation to a single load point.

5. GEOMETRICAL LIMITS OF VECTOR FIELD

Since the existing dimensions of the Dynaflect make it inconvenient to measure vertical displacements at locations closer than x = 0 (or r = 10 inches) from the load application points, or horizontal displacements at locations closer than x = 6 inches (or r = 11.7 inches), these dimensions form the close-in limits of the measured displacement fields. The far-out limit of x = 216 inches (or r = 216.2 inches) was selected upon consideration of the finite (40 ft.) length of the sections and the observed diminution of the displacements with distance and with depth. The deep limit, at $z \approx 65$ inches below the surface, was selected on the basis that the test facility comprises 53 inches of selected materials on a reasonably uniform clay foundation which is regarded as extending infinitely downward. In view of the observed displacement behavior it is believed that the outer limits of the measured fields have been placed amply far to encompass the region of major interest and to permit reasonable extrapolation beyond this region.

Thus, the geometrical limits of the transformed vector fields determined from the measurements are as follows:

Field of the component u -

$11.7 \text{ in.} \leq r \leq 216.2 \text{ in.}, \; 0 \leq z \leq 65 \text{ in.}$ (approx.)

Field of the component w -

$10 \text{ in.} \leq r \leq 216.2 \text{ in.}, \; 0 \leq z \leq 65 \text{ in.}$ (approx.)

6. MEASURED DISPLACEMENTS

Replicate measurements of displacements have been made on three pavement sections and are shown in Figures 11, 12 and 13. In each of these figures the layer thicknesses determined in the measurement holes are shown at the top, contours of equal vertical displacement, w, are shown in the center, and contours of equal horizontal displacement, u, are shown at the bottom. The data used to prepare these figures are given in Appendix A.

Observed w values are positive everywhere in all plots; thus all points had a component of motion downward. Both positive and negative values were found for u. Positive values indicate a component of motion directed outward from the load axis; negative values indicate motion toward it.

For all three sections the fields shown for replication 1 are very similar to those for replication 2. The differences between the replications are quite small in comparison to the differences between sections. The main difference between sections that can be seen in the w fields is in the magnitude near the load. More striking differences between sections appear in the u-fields. The general magnitude of the displacements in the three sections shown are clearly related to the designs; that is, the magnitudes are in inverse order of pavement strength.

Figure 14 shows w and u fields for two assumed homogeneous elastic half-spaces which have values of Poisson's ratio of 0.5 and 0.25 respectively. To prepare these fields, displacements were calculated using the point load equations for w and u given in Reference 11. The vertical

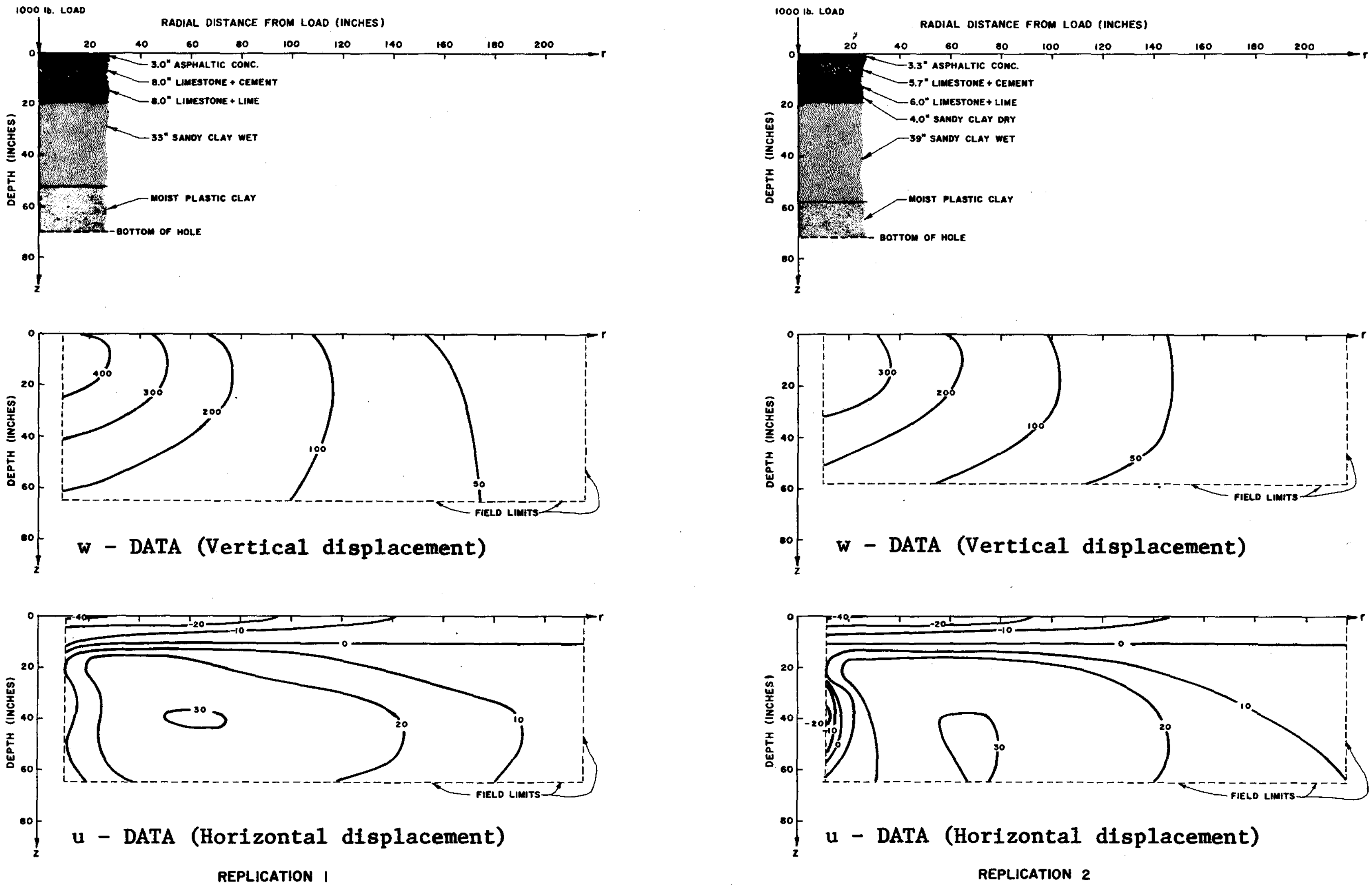

Figure 11: Displacement fields measured in section 25. Numerical values on contours denote displacements in microinches (inches x 10^{-6}).

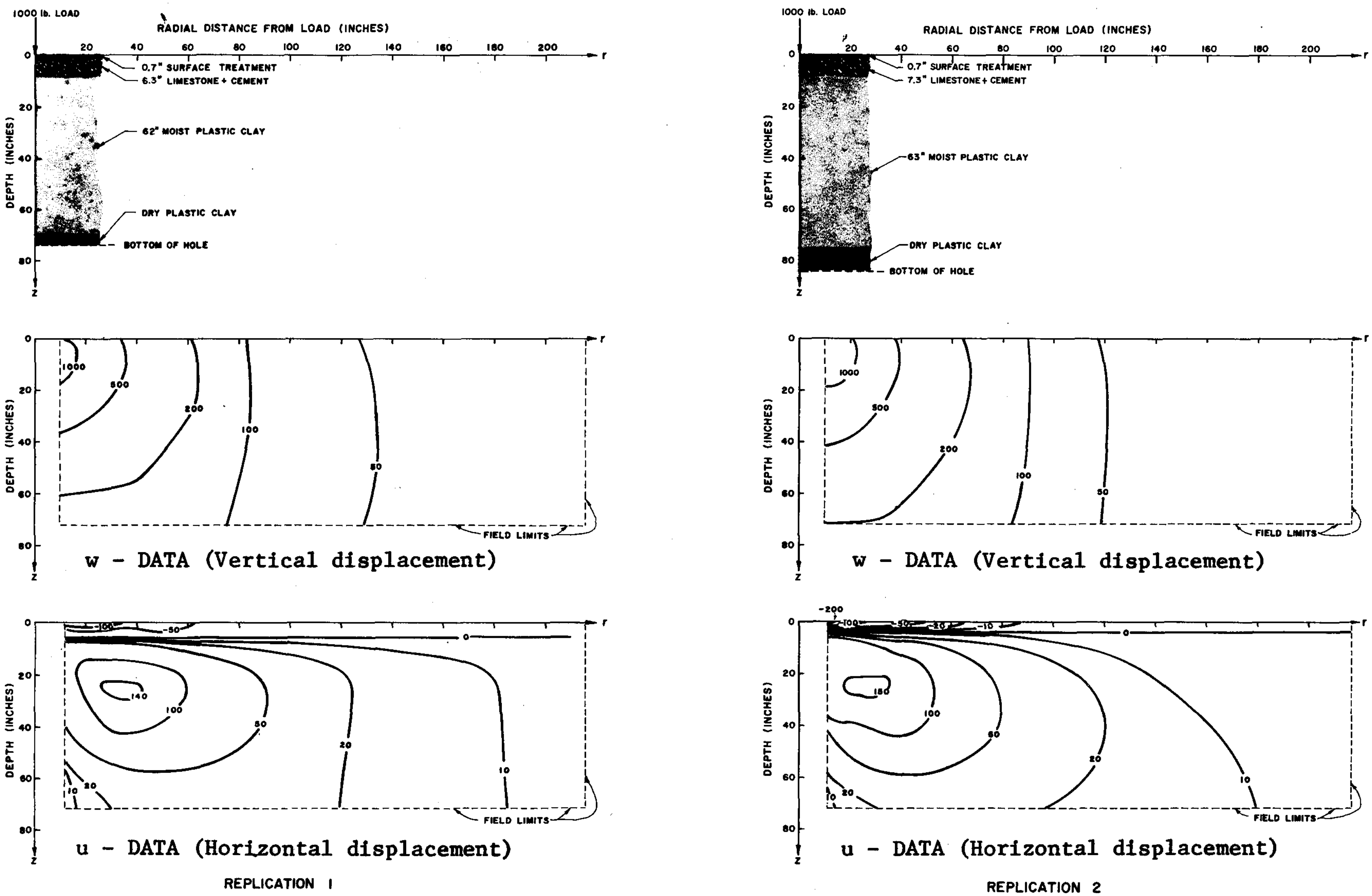

Figure 12: Displacement fields measured in section 31. Numerical values on contours denote displacements in microinches (inches x 10^{-6}).

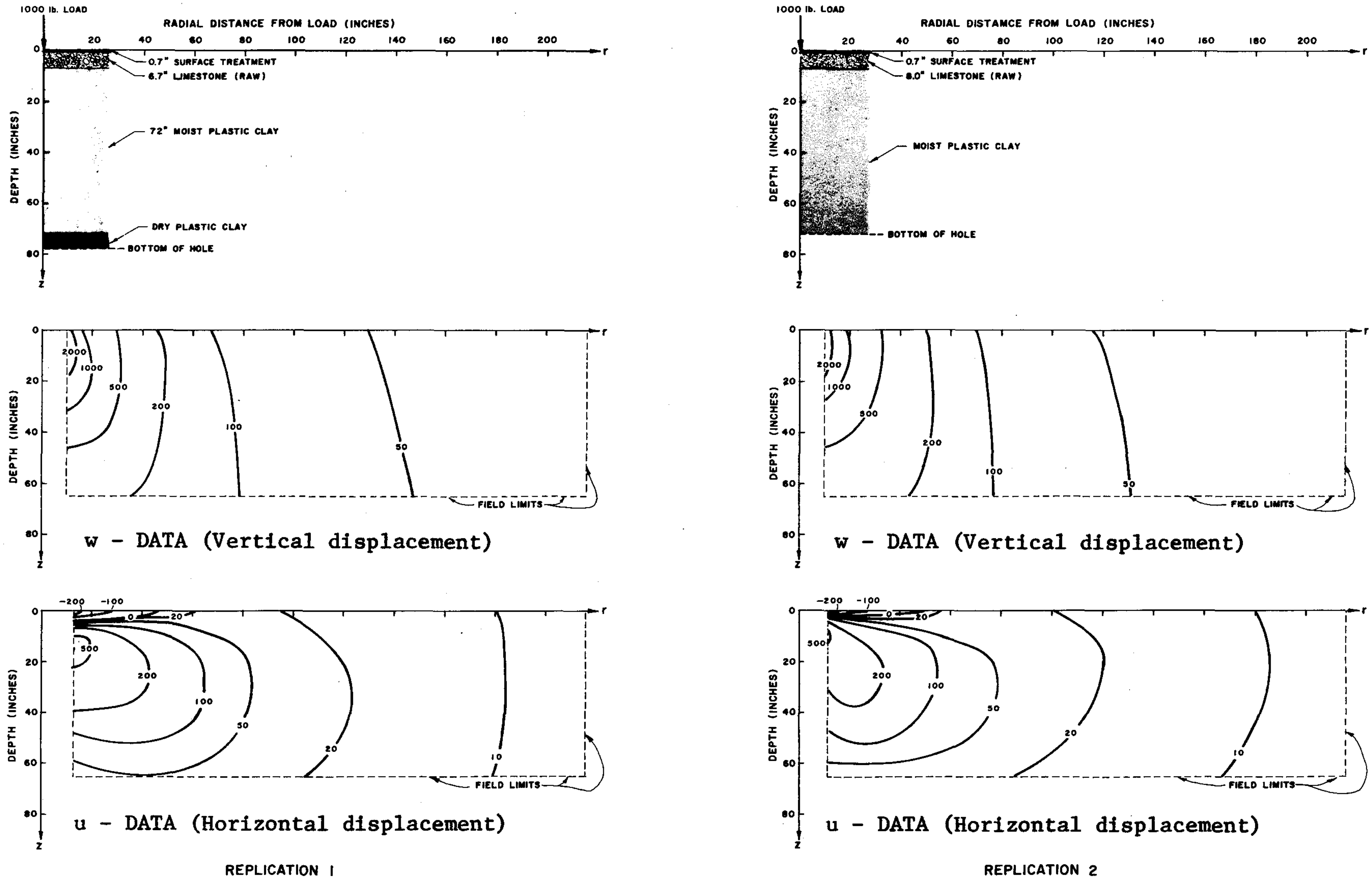

Figure 13: Displacement fields measured in section 32. Numerical values on contours denote displacements in microinches (inches x 10^{-6}).

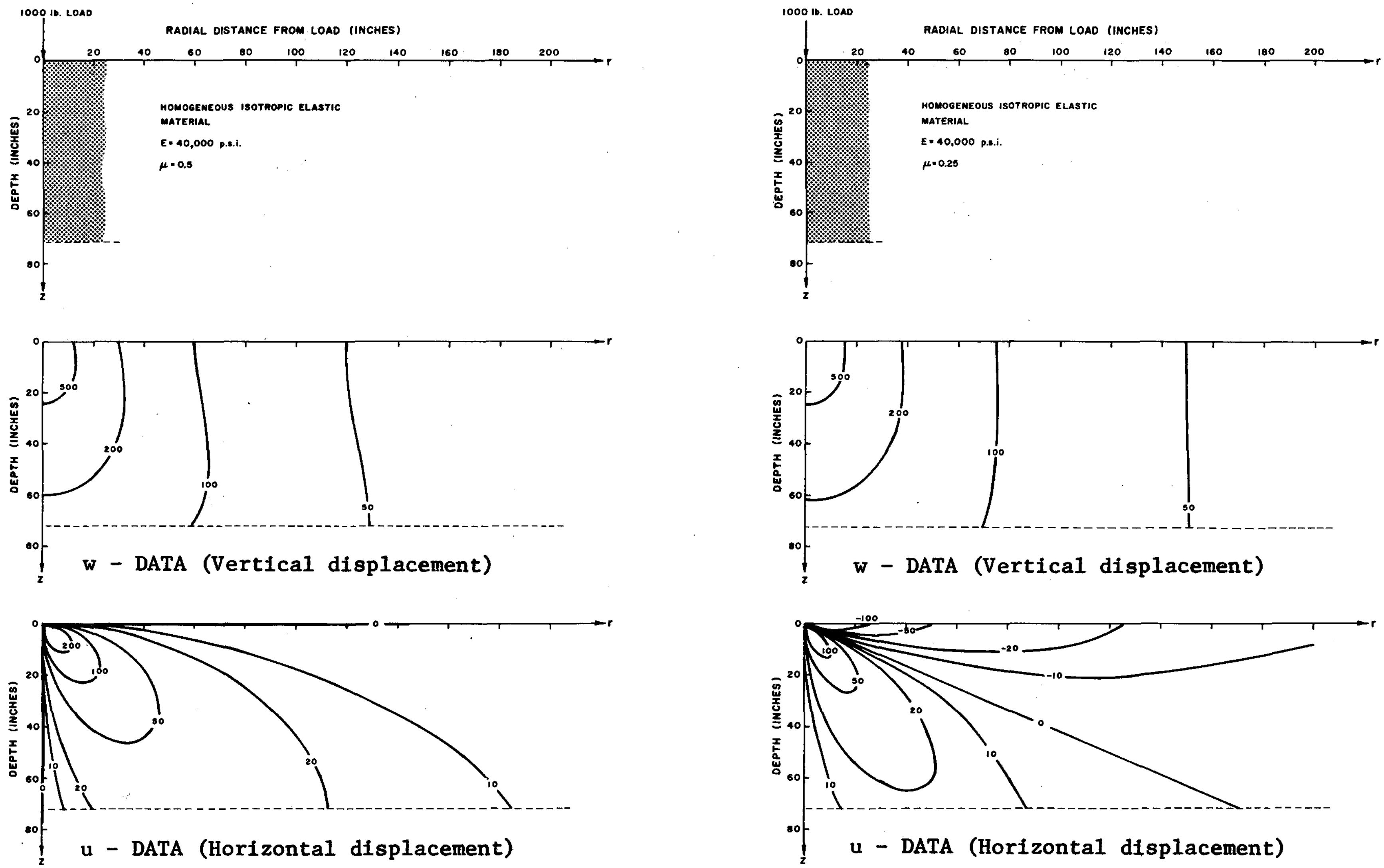

Figure 14: Computed displacement fields for homogeneous isotropic elastic half spaces. Numerical values on contours denote displacements in microinches (inches x 10^{-6}).

displacement is positive everywhere for both cases; however, the horizontal displacement is positive everywhere only for the limiting case of Poisson's ratio equal to 0.5. When Poisson's ratio has any value less than 0.5 a negative region occurs near the surface.

Figure 15 shows w and u fields for a pair of two-layer elastic systems. The two cases differ in that one is for Poisson's ratio equal to 0.5 in both layers and the other is for Poisson's ratio equal to 0.25 in both layers. Both cases are for a 19 inch thick top layer having an elastic modulus of 600,000 psi above an infinitely thick layer having an elastic modulus of 20,000 psi. The dimension of 19 inches was chosen to match the total design pavement thickness (depth to top of embankment) of section 25. The displacements shown were calculated by using a computer program developed by the Chevron Oil Company (12, 13) using a 1000 lb. load on a circular area having a radius of 1.41 inches. The radius approximates that of the contact area of a Dynaflect load wheel (14).

The measurements made on section 25, Figure 1, are somewhat similar to the fields computed for the two-layer elastic systems illustrated in Figure 15. The general shapes of both the u and the w fields are alike and the position of the zero contour for u in both cases is approximately horizontal and about 10 inches from the pavement surface. Work toward developing elastic layered system fields to match the observed fields is continuing.

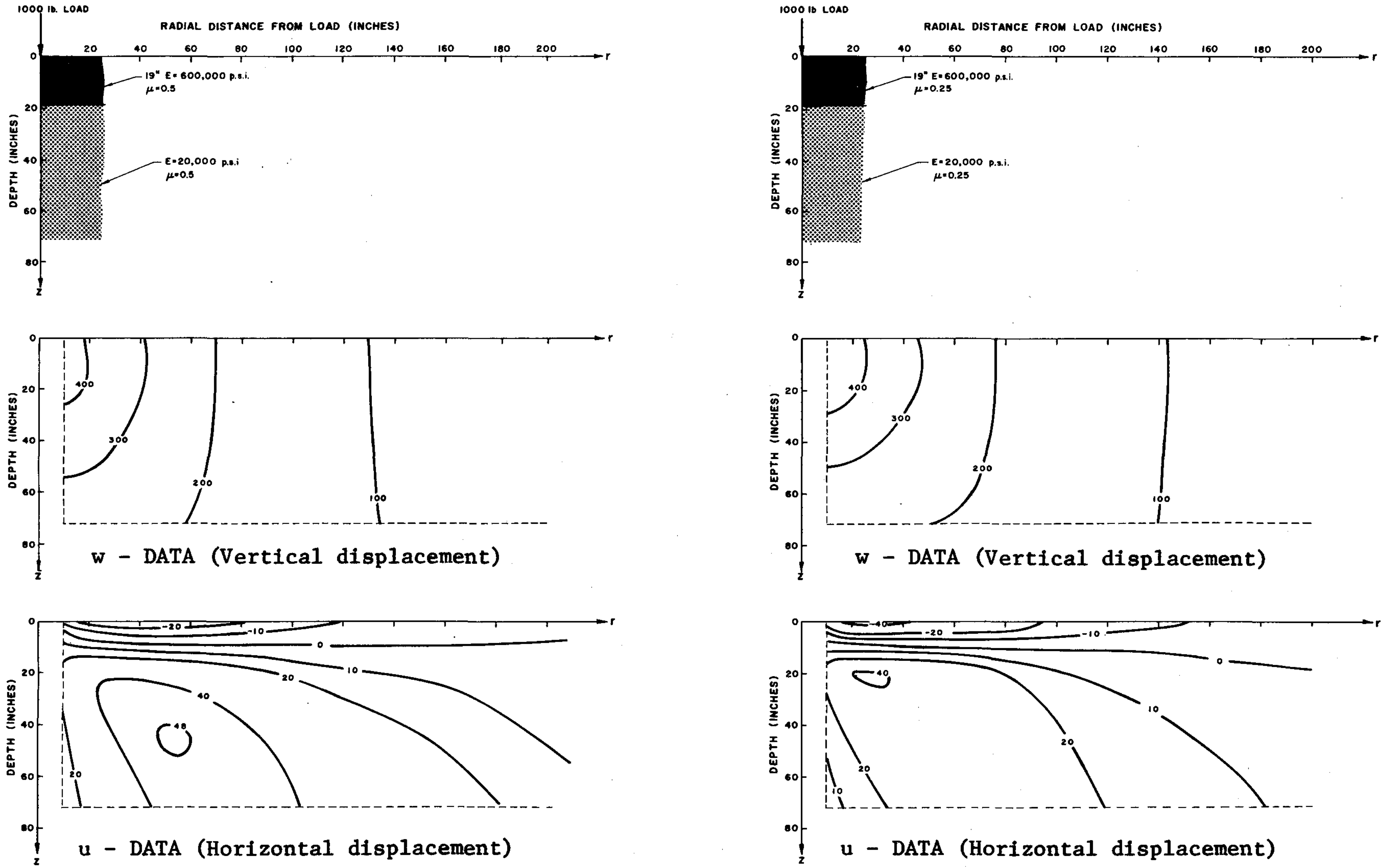

Figure 15: Computed displacement fields for two-layer elastic systems. Numerical values on contours denote displacements in microinches (inches x 10^{-6}).

7. REPLICATION ERRORS

As previously mentioned, replicate measurements were made on opposite ends of a test section and their differences generally were found to be quite small when compared with differences between sections, as evidenced by Figures 11, 12 and 13. The differences between the measurements made on the same section are due to both the variability of the measuring process as well as the variability in the structural characteristics of the section at its two ends. In the measurement procedure used, all points were not replicated. Thus, in the determination of the replication errors only the points which were replicated could be compared.

Plots of the replication errors (half the difference between the observations) versus the mean observation (half the sum of the observations) are shown in Figures 16, 17 and 18. Also shown on these plots are the percentage error lines which include three-fourths of the replication errors. As can be seen in these figures the data are somewhat biased as indicated by sloping trends in many of the plots. This indicates a consistant difference between the two ends of a section. Nevertheless when disregarding the reasons for the errors, the errors found in w are very small when compared to the range of the measured values and the errors found in u are thought to be acceptable. The larger percentage errors found in u are chiefly due to the fact that the relative magnitude of u changes much more rapidly within the measured field than does the relative magnitude of w. This is evidenced by the crowding of the contour lines in the plots of the u-fields, Figures 11, 12 and 13.

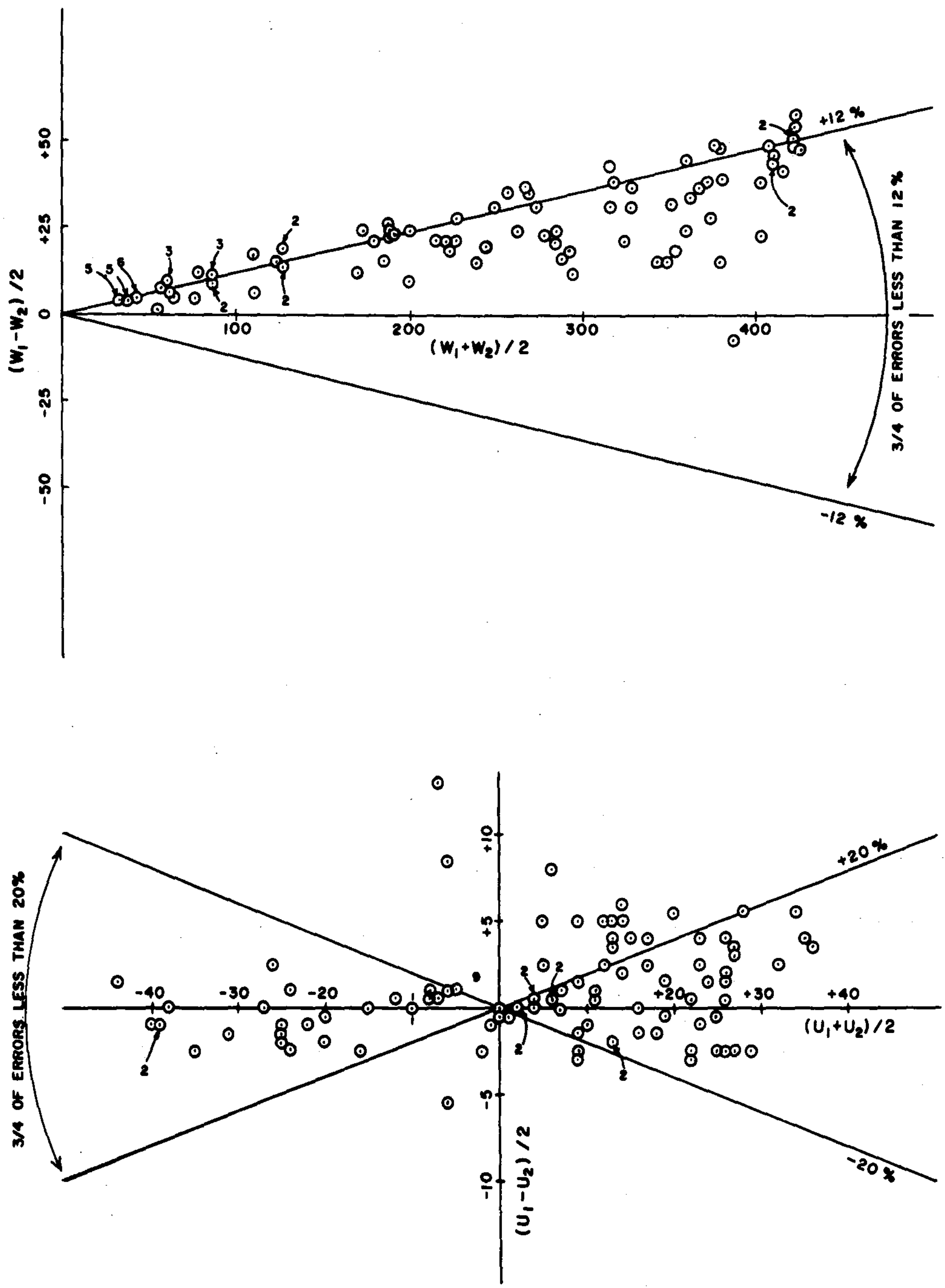

Figure 16: Replication errors for section 25 (half the difference between observations) versus mean observations. Scales are in microinches. Multiple occurrences of points are indicated by number.

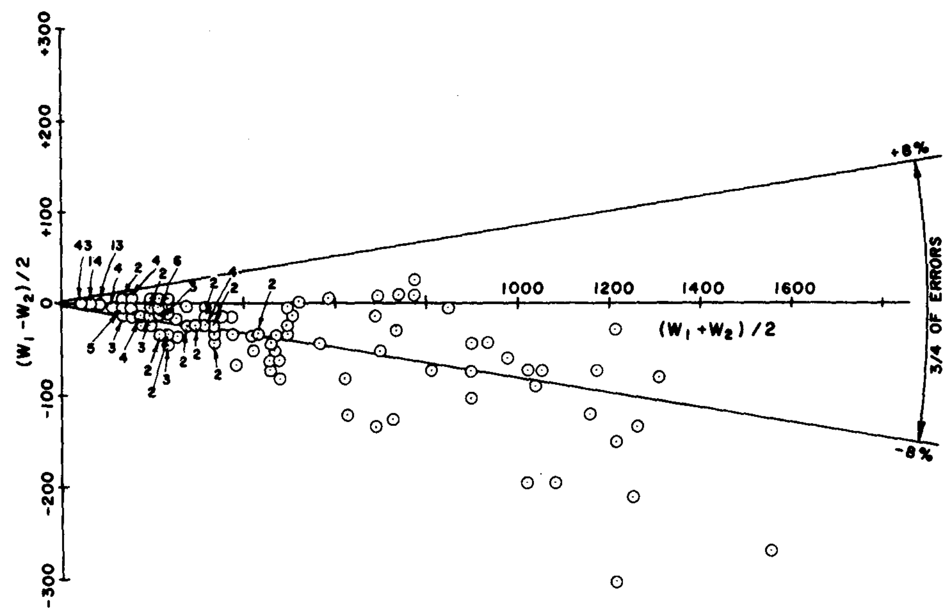

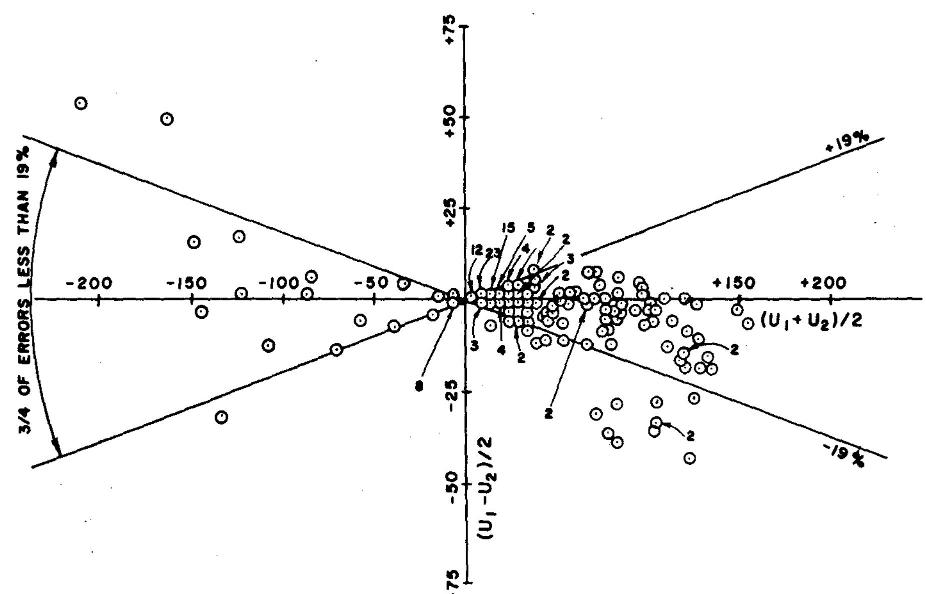

Figure 17: Replication errors for section 31 (half the difference between observations) versus mean observations. Scales are in microinches. Multiple occurrences of points are indicated by number.

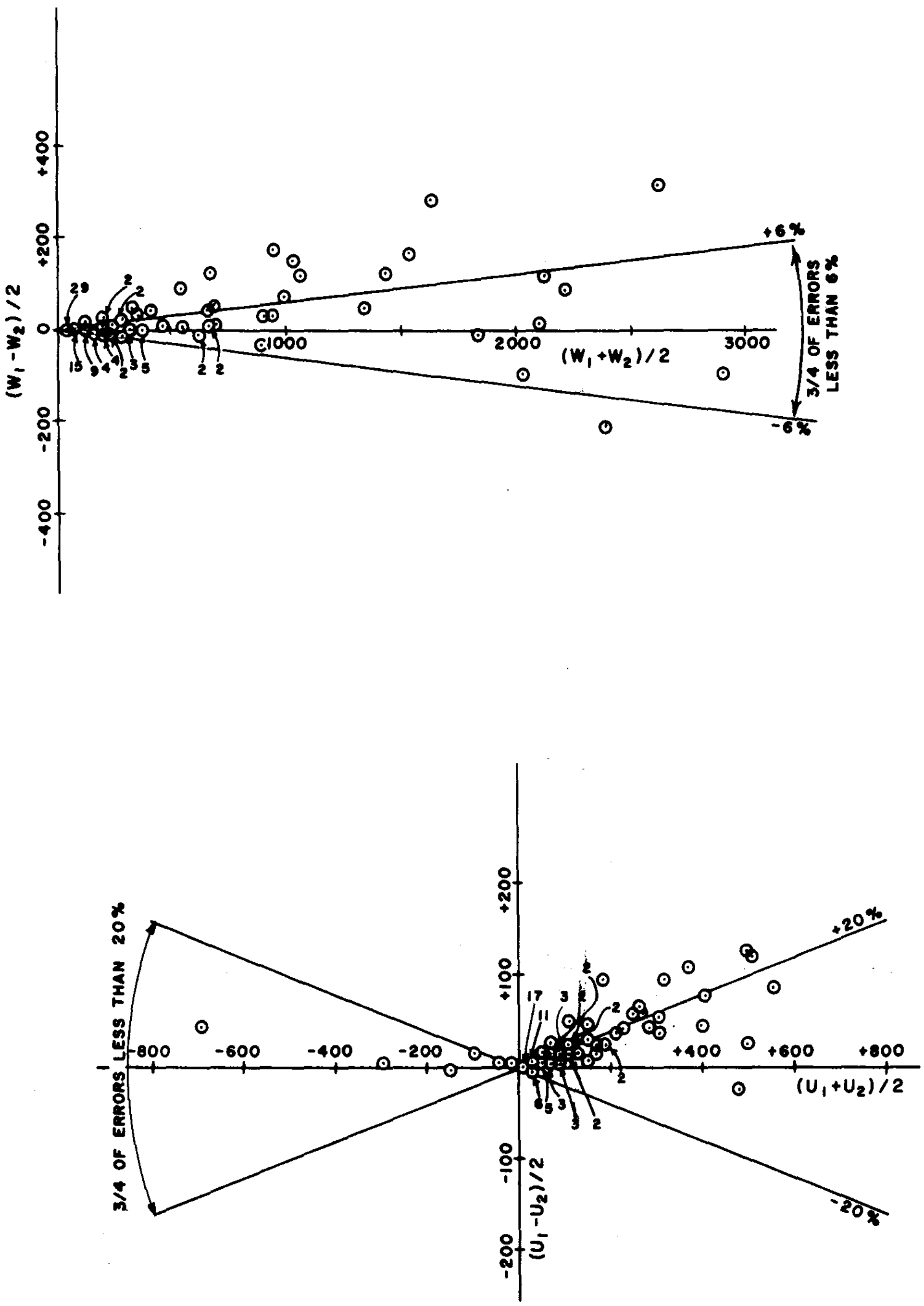

Figure 18: Replication errors for section 32 (half the difference between observations) versus mean observations. Scales are in microinches. Multiple occurrences of points are indicated by number.

Table 1 is a summary of the replication measurements. It shows the average, the average absolute, and the range of the mean observations. From these values one can note that the sections measured were very different. The table also contains the maximum absolute and the root mean square of the replication errors as well as the percentage error values which will include half and three-fourths of the errors. Values in the last column are displayed graphically in Figures 16, 17 and 18.

Table 1: Summary of Replication Measurements

Section	Variable Measured	Number of Comparisons	Mean Observation[1]			Replication Error[2]		Percent Error[3]	
			Average	Average Absolute	Range	Maximum Absolute	Root Mean Square	1/2 of Errors <	3/4 of Errors <
25	w	98	223.6	223.6	31 to 424	57	26.4	10	12
25	u	104	4.1	15.6	-44 to 36	13	2.9	10	20
31	w	196	301.4	301.4	30 to 1545	303	52.8	5	8
31	u	182	33.4	51.3	-210 to 166	97	13.6	10	19
32	w	112	433.9	433.9	30 to 2912	307	60.9	3	6
32	u	89	94.6	123.4	-686 to 556	126	34.0	13	20

[1] Mean of two replicated observations, $(w_1 + w_2)/2$ or $(u_1 + u_2)/2$.

[2] One half of the difference between two replicated observations, $(w_1 - w_2)/2$ or $(u_1 - u_2)/2$.

[3] Replication error divided by mean observation, expressed as a percentage.

8. CONCLUSIONS

From the results to date in this study the following conclusions appear warranted:

1. A practical fieldworthy measuring technique has been developed for use with the Dynaflect to observe the displacement vector throughout the body of a pavement section.
2. Replication errors observed on a test section are reasonably small compared to variations between sections.
3. The observed vector displacement fields resemble fields computed for a layered elastic system to which an equal static load is applied.
4. It appears feasible to determine for each section a set of elastic layers for which the computed displacement fields will substantially match the observations.
5. Examination of the data indicates that it should be possible to formulate a useful and practical mathematical model representing the displacement response of the several pavement sections.

9. REFERENCES

1. Scrivner, F. H. and Moore, W. M. "Evaluation of the Stiffness of Individual Layers in a Specially Designed Pavement Facility from Surface Deflections," Research Report 32-8, Texas Transportation Institute, Texas A&M University, College Station, Texas, 1966.

2. Scrivner, F. H. and Moore, W. M. "An Empirical Equation for Predicting Pavement Deflections," Research Report 32-12, Texas Transportation Institute, Texas A&M University, College Station, Texas, 1968.

3. Scrivner, F. H.; Moore, W. M.; McFarland, W. F., and Carey, G. R. "A Systems Approach To The Flexible Pavement Design Problem," Research Report 32-11, Texas Transportation Institute, Texas A&M University, College Station, Texas, 1968.

4. Hudson, R. W.; McCullough B. F.; Scrivner, F. H. and Brown, J. L. "A Systems Approach Applied to Pavement Design and Research," Research Report 123-1, Texas Transportation Institute, Texas A&M University, College Station, Texas, 1970.

5. Brown, S. F. and Pell, P. S. "An Experimental Investigation of the Stresses, Strains, and Deflections in a Layered Pavement Structure Subjected to Dynamic Loads," Proceedings of the Second International Conference on the Structural Design of Asphalt Pavements, University of Michigan, Ann Arbor, Michigan, 1967, pp. 487-504.

6. Gusfeldt, K. H. and Dempwolff, K. R. "Stress and Strain Measurements in Experimental Road Sections Under Controlled Loading Conditions," Proceedings of the Second International Conference on the Structural Design of Asphalt Pavements, University of Michigan, Ann Arbor, Michigan, 1967, pp. 663-669.

7. Klomp, A. J. G. and Niesman, TH. W. "Observed and Calculated Strains at Various Depths in Asphalt Pavements," Proceedings of the Second International Conference on the Structural Design of Asphalt Pavements, University of Michigan, Ann Arbor, Michigan, 1967, pp. 671-688.

8. Nijboer, L. W. "Testing Flexible Pavements Under Normal Traffic Loadings by Means of Measuring Some Physical Quantities Related to Design Theories," Proceedings of the Second International Conference on the Structural Design of Asphalt Pavements, University of Michigan, Ann Arbor, Michigan, 1967, pp. 689-705.

9. Scrivner, F. H.; Swift, Gilbert; and Moore, W. M. "A New Research Tool for Measuring Pavement Deflection," Highway Research Record No. 129, Washington, D. C., pp. 1-11, 1966.

10. Pace, George M. "Evaluation of the Dynaflect for the Non-Destructive Testing of Portland Cement Concrete Pavements," Technical Report No. 4-61, Department of the Army, Ohio Division Laboratories, Corps of Engineers, Cincinnati, Ohio, 1967.

11. Timoshinko, S. and Goodier, J. N. Theory of Elasticity, McGraw Hill Book Co., Inc., 1951, pp. 33 & 365.

12. Michelow, J. "Analysis of Stresses and Displacements in an N-Layered Elastic System Under a Load Uniformly Distributed over a Circular Area," California Research Corporation, Richmond, California, September, 1963.

13. Warren, H. and Dieckmann, W. L. "Numerical Computation of Stresses and Strains in a Multiple-Layered Asphalt Pavement System," California Research Corporation, Richmond, California, September, 1963.

14. Scrivner, F. H., Michalak, C. H. and Moore, W. M. "Calculation of the Elastic Moduli of a Two Layer Pavement System from Measured Surface Deflections," Research Report Number 123-6, Texas Transportation Institute, Texas A&M University, College Station, Texas, 1971.

APPENDIX A

Included in this appendix are lists of the components, w and u respectively, for three pavement sections. These values are measurements transformed to represent values which would have been observed for a single load point as explained in Section 4. The drilling record for each measurement hole is also given.

SECTION 25 REPLICATION 1

W - DATA (MICRO-INCHES) FOR SINGLE 1000 LB. LOAD

DEPTH Z (IN.)	*************** R A D I A L					D I S T A N C E R				(I N .) ***************				
	10.0	11.7	15.6	20.6	26.0	37.4	49.0	60.8	72.7	96.5	120.4	144.3	180.3	216.2
0.0	378	424	393	363	357	306	263	209	181	118	81	56	40	33
3.0	469	469	454	424	403	354	303	242	212	145	96	69	48	39
11.0	478	475	454	424	399	345	303	242	212	142	93	66	48	36
15.0	469	469	451	424	403	357	303	248	212	145	96	69	48	39
19.0	451	454	439	409	393	345	303	254	215	142	96	69	48	39
29.0	381	381	369	363	357	309	278	236	199	139	96	66	48	39
41.0	303	299	299	290	284	254	224	196	175	127	90	69	45	36
52.0	230	230	224	218	212	196	178	157	139	109	81	63	45	36
65.0	193	193	187	187	187	175	163	145	133	103	81	63	48	36

D R I L L I N G L O G D A T A

LAYER NO.	DEPTH Z (IN.) FROM	TO	**** MATERIAL ****
1	0.0	3.0	ASPHALTIC CONCRETE
2	3.0	11.0	LIMESTONE + CEMENT
3	11.0	19.0	LIMESTONE + LIME
4	19.0	52.0	SANDY CLAY, WET
5	52.0	70.0	PLASTIC CLAY, MOIST

SECTION 25 REPLICATION 1

U - DATA (MICRO-INCHES) FOR SINGLE 1000 LB. LOAD

DEPTH Z (IN.)	10.0	11.7	15.6	20.6	26.0	37.4	49.0	60.8	72.7	96.5	120.4	144.3	180.3	216.2
	*************** R A D I A L				D I S T A N C E			R	(I N .)		**************			
0.0		-42	-38	-40	-39	-39	-37	-32	-26	-20	-14	-10	-7	-5
3.0		-24	-22	-25	-26	-26	-26	-23	-21	-18	-11	-7	-5	-4
11.0		-11	-4	-2	0	0	0	0	0	0	0	0	0	0
15.0		8	13	16	17	19	18	16	14	10	6	4	1	0
19.0		9	18	21	24	26	27	25	22	16	11	7	4	1
29.0		2	10	16	20	27	30	30	29	25	19	15	7	4
41.0		5	13	20	25	33	39	39	39	34	28	20	12	7
52.0		3	10	16	21	28	33	35	35	32	26	21	12	8
65.0		5	6	10	14	18	24	25	26	24	19	15	10	7

D R I L L I N G L O G D A T A

LAYER NO.	DEPTH Z (IN.) FROM	TO	**** MATERIAL ****
1	0.0	3.0	ASPHALTIC CONCRETE
2	3.0	11.0	LIMESTONE + CEMENT
3	11.0	19.0	LIMESTONE + LIME
4	19,0	52.0	SANDY CLAY, WET
5	52.0	70.0	PLASTIC CLAY, MOIST

SECTION 25 REPLICATION 2

W - DATA (MICRO-INCHES) FOR SINGLE 1000 LB. LOAD

DEPTH Z (IN.)	RADIAL DISTANCE R (IN.) 10.0	11.7	15.6	20.6	26.0	37.4	49.0	60.8	72.7	96.5	120.4	144.3	180.3	216.2
0.0	393	378	363	333	327	281	224	190	157	106	72	54	36	28
3.0	378	372	357	333	315	278	230	206	163	106	72	57	39	31
11.0	363	366	363	345	345	284	242	199	166	115	78	56	39	31
15.0	369	369	363	330	330	272	233	206	169	109	75	54	36	30
19.0	363	372	363	333	327	303	254	199	163	115	78	60	39	31
29.0	318	333	333	290	296	272	218	193	169	109	72	51	39	30
41.0	260	266	254	221	236	224	175	148	133	93	66	51	36	28
58.0	166	166	151	145	142	133	109	96	89	69	48	37	31	27

DRILLING LOG DATA

LAYER NO.	DEPTH Z (IN.) FROM	TO	**** MATERIAL ****
1	0.0	3.3	ASPHALTIC CONCRETE
2	3.3	9.0	LIMESTONE + CEMENT
3	9.0	15.0	LIMESTONE + LIME
4	15.0	19.0	SANDY CLAY, DRY
5	19.0	58.0	SANDY CLAY, WET
6	58.0	72.0	PLASTIC CLAY, MOIST

SECTION 25 REPLICATION 2

U - DATA (MICRO-INCHES) FOR SINGLE 1000 LB. LOAD

DEPTH Z (IN.)	************** R A D I A L					D I S T A N C E		R		(I N .) **************				
	10.0	11.7	15.6	20.6	26.0	37.4	49.0	60.8	72.7	96.5	120.4	144.3	180.3	216.2
0.0		-45	-38	-38	-38	-38	-33	-29	-26	-19	-14	-10	-8	-7
3.0		-28	-24	-23	-23	-22	-21	-20	-17	-13	-11	-8	-7	-5
11.0		0	0	0	0	0	0	0	0	0	0	0	0	0
15.0		2	3	6	7	9	10	8	8	7	5	2	2	1
19.0		11	19	23	25	25	24	22	20	16	10	5	2	1
29.0		-14	0	10	12	19	22	23	23	20	14	11	5	4
41.0		-20	-1	8	14	22	28	31	32	29	23	17	10	7
58.0		2	3	11	14	21	25	28	31	28	23	20	14	9
65.0		11	11	14	17	24	28	29	31	29	25	19	14	10

D R I L L I N G L O G D A T A

LAYER NO.	DEPTH Z (IN.) FROM	TO	**** MATERIAL ****
1	0.0	3.3	ASPHALTIC CONCRETE
2	3.3	9.0	LIMESTONE + CEMENT
3	9.0	15.0	LIMESTONE + LIME
4	15.0	19.0	SANDY CLAY, DRY
5	19.0	58.0	SANDY CLAY, WET
6	58.0	72.0	PLASTIC CLAY, MOIST

SECTION 31 REPLICATION 1

W - DATA (MICRO-INCHES) FOR SINGLE 1000 LB. LOAD

DEPTH Z (IN.)	RADIAL DISTANCE R (IN.) 10.0	11.7	15.6	20.6	26.0	37.4	49.0	60.8	72.7	96.5	120.4	144.3	180.3	216.2
0.0	1212	909	818	787	696	409	287	206	133	69	51	40	33	31
0.7	1272	1030	1030	909	772	484	318	196	145	72	56	45	39	33
4.0	1060	999	909	909	787	484	303	212	145	74	53	45	36	33
8.0	1121	1060	969	818	787	469	284	206	124	63	51	42	33	30
12.0	1090	1060	1030	909	787	499	296	236	151	75	57	48	39	33
13.0	1181	878	939	848	742	409	290	218	145	72	54	45	36	33
17.0	1090	939	878	833	696	424	303	187	145	75	54	45	36	31
24.0	727	590	545	636	581	363	260	215	142	81	53	46	39	31
29.0	666	499	530	515	515	333	242	196	139	87	60	42	36	28
36.0	484	393	454	409	393	318	263	193	139	90	63	48	34	31
41.0	381	381	390	363	342	260	224	169	130	90	63	48	36	30
48.0	309	290	290	303	303	212	187	151	121	84	57	45	33	28
53.0	303	290	290	290	248	224	184	145	109	81	57	45	36	30
60.0	184	187	193	187	236	181	157	127	115	75	57	46	33	31
65.0	181	169	184	206	199	157	148	127	109	72	54	45	33	30
72.0	145	157	163	184	187	139	127	127	103	69	63	48	33	31

DRILLING LOG DATA

LAYER NO.	DEPTH Z (IN.) FROM	TO	**** MATERIAL ****
1	0.0	0.7	SURFACE TREATMENT
2	0.7	8.0	LIMESTONE + CEMENT
3	8.0	70.0	PLASTIC CLAY, MOIST
4	70.0	74.0	PLASTIC CLAY, DRY

SECTION 31 REPLICATION 1

U - DATA (MICRO-INCHES) FOR SINGLE 1000 LB. LOAD

DEPTH Z (IN.)	*************** R A D I A L					D I S T A N C E		R	(I N .)	****************				
	10.0	11.7	15.6	20.6	26.0	37.4	49.0	60.8	72.7	96.5	120.4	144.3	180.3	216.2
0.0		-157	-133	-148	-165	-85	-84	-47	-23	-8	-11	-7	-5	-8
0.7		-114	-107	-121	-121	-73	-63	-29	-14	-5	-11	-7	-5	-5
4.0		-57	-42	-43	-38	-33	-25	-19	-13	-13	-10	-10	-8	-7
8.0		68	76	67	57	39	25	20	16	11	8	7	7	5
12.0		57	76	84	84	82	69	47	37	20	10	8	5	2
13.0		68	88	94	95	88	72	53	41	22	11	10	10	7
17.0		40	95	107	114	119	99	74	62	32	14	10	7	4
24.0		68	99	127	146	143	123	98	75	45	23	12	9	8
29.0		41	66	97	114	115	111	98	77	47	23	14	9	8
36.0		34	57	74	98	103	105	86	68	44	23	14	10	7
41.0		51	68	80	98	106	96	84	74	47	23	14	10	8
48.0		27	42	52	63	76	76	68	57	39	23	14	10	8
53.0		20	36	42	47	64	64	61	53	36	21	15	10	8
60.0		5	17	23	25	36	40	40	37	29	20	15	10	10
65.0		6	13	16	22	28	34	35	32	28	20	15	11	10
72.0		5	11	15	19	24	30	31	29	26	20	16	11	10

D R I L L I N G   L O G   D A T A

LAYER NO.	DEPTH Z (IN.) FROM	TO	**** MATERIAL ****
1	0.0	0.7	SURFACE TREATMENT
2	0.7	8.0	LIMESTONE + CEMENT
3	8.0	70.0	PLASTIC CLAY, MOIST
4	70.0	74.0	PLASTIC CLAY, DRY

SECTION 31 REPLICATION 2

W - DATA (MICRO-INCHES) FOR SINGLE 1000 LB. LOAD

DEPTH Z (IN.)	*************** R A D I A L D I S T A N C E R (I N .) ***************													
	10.0	11.7	15.6	20.6	26.0	37.4	49.0	60.8	72.7	96.5	120.4	144.3	180.3	216.2
0.0	1393	1515	1212	999	757	499	333	224	136	74	46	43	36	30
0.7	1818	1454	1272	1030	757	499	333	224	136	75	48	43	36	30
8.0	1393	1363	1121	969	742	515	333	224	115	72	48	43	36	31
13.0	1242	1272	1090	939	727	530	333	224	142	78	51	45	36	30
17.0	1242	1121	969	848	681	499	327	206	139	78	53	46	36	31
24.0	878	848	818	742	575	469	303	212	139	84	54	45	37	33
29.0	696	742	696	606	515	393	290	212	133	90	54	46	37	31
36.0	515	560	530	515	454	363	275	206	139	87	57	48	36	31
41.0	530	515	454	442	381	306	254	190	130	84	56	48	36	30
48.0	448	384	372	360	318	290	224	172	121	87	57	48	36	31
53.0	363	348	333	312	303	263	218	163	124	90	60	51	37	31
60.0	287	284	278	266	233	206	175	151	118	84	60	49	36	30
65.0	260	242	248	224	212	212	175	151	109	84	60	51	36	31
72.0	199	196	199	199	181	172	151	133	106	81	57	48	36	31

D R I L L I N G L O G D A T A

LAYER NO.	DEPTH Z (IN.) FROM	TO	**** MATERIAL ****
1	0.0	0.7	SURFACE TREATMENT
2	0.7	8.0	LIMESTONE + CEMENT
3	8.0	75.0	PLASTIC CLAY, MOIST
4	75.0	84.0	PLASTIC CLAY, DRY

SECTION 31 REPLICATION 2

U - DATA (MICRO-INCHES) FOR SINGLE 1000 LB. LOAD

DEPTH Z (IN.)	10.0	11.7	15.6	20.6	26.0	37.4	49.0	60.8	72.7	96.5	120.4	144.3	180.3	216.2
	****************** R A D I A L				D I S T A N C E			R (I N .)				******************		
0.0		-262	-164	-141	-101	-88	-57	-32	-14	-7	-6	-3	-4	-7
0.7		-211	-141	-124	-95	-85	-52	-38	-16	-8	-7	-4	-10	-11
8.0		262	164	134	98	64	48	26	20	9	8	4	4	8
13.0		85	103	107	101	94	78	56	35	16	11	5	5	5
17.0		102	122	144	137	119	105	74	50	23	14	7	6	7
24.0		137	137	158	159	149	126	92	68	29	17	8	7	7
29.0		120	137	151	152	146	129	89	62	32	17	9	6	9
36.0		108	114	131	133	134	117	89	65	32	19	12	7	8
41.0		48	80	87	101	106	93	80	59	32	19	12	8	8
48.0		40	49	77	82	88	84	68	53	32	20	12	8	8
53.0		31	45	50	60	64	66	56	47	29	19	13	8	8
60.0		20	30	37	43	48	48	46	38	26	18	12	7	5
65.0		3	16	21	25	36	39	29	23	17	13	12	10	8
72.0		2	11	16	19	27	33	28	24	20	14	12	11	8

D R I L L I N G L O G D A T A

LAYER NO.	DEPTH Z (IN.) FROM	TO	**** MATERIAL ****
1	0.0	0.7	SURFACE TREATMENT
2	0.7	8.0	LIMESTONE + CEMENT
3	8.0	75.0	PLASTIC CLAY, MOIST
4	75.0	84.0	PLASTIC CLAY, DRY

SECTION 32 REPLICATION 1

W - DATA (MICRO-INCHES) FOR SINGLE 1000 LB. LOAD

DEPTH Z (IN.)	10.0	11.7	15.6	20.6	26.0	37.4	49.0	60.8	72.7	96.5	120.4	144.3	180.3	216.2
	*************** RADIAL DISTANCE R (IN.) ***************													
0.0	2823	2117	1382	852	617	323	194	126	94	67	55	47	38	29
1.5	2676	2529	1705	999	661	352	194	123	88	64	49	41	35	27
6.7	2823	2294	1705	970	676	338	182	123	94	69	54	47	35	29
13.0	2176	2235	1911	1058	735	382	205	129	94	70	55	47	38	32
17.0	1941	1823	1558	941	676	352	205	129	94	67	55	47	35	29
29.0	1176	1176	1117	794	617	367	217	147	105	73	55	44	38	29
41.0	617	705	691	558	470	323	211	147	108	76	58	49	36	29
53.0	382	397	441	352	323	247	191	141	111	82	58	49	38	29
65.0	255	258	294	247	235	194	161	129	105	82	61	49	36	32

D R I L L I N G L O G D A T A

LAYER NO.	DEPTH Z (IN.) FROM	TO	**** MATERIAL ****
1	0.0	0.7	SURFACE TREATMENT
2	0.7	6.7	LIMESTONE (RAW)
3	6.7	72.0	PLASTIC CLAY, MOIST
4	72.0	78.0	PLASTIC CLAY, DRY

SECTION 32 REPLICATION 1

U - DATA (MICRO-INCHES) FOR SINGLE 1000 LB. LOAD

DEPTH Z (IN.)	************** R A D I A L					D I S T A N C E			R	(I N .)		**************		
	10.0	11.7	15.6	20.6	26.0	37.4	49.0	60.8	72.7	96.5	120.4	144.3	180.3	216.2
0.0		-643	-290	-86	-150	-40	-14	20	30	18	15	12	NR	NR
1.5		-292	-235	-58	-68	18	15	30	22	18	12	NR	NR	NR
6.7		444	313	275	156	90	64	42	27	21	15	12	NR	NR
13.0		526	627	482	326	200	129	91	57	24	18	12	NR	NR
17.0		643	627	482	358	250	153	91	72	30	18	12	NR	NR
29.0		327	360	344	326	265	184	128	82	39	22	13	NR	NR
41.0		163	180	206	205	190	141	109	76	39	21	15	9	NR
53.0		70	86	103	110	112	92	70	48	30	18	12	NR	NR
65.0		26	27	41	45	50	49	36	33	23	16	12	NR	NR

D R I L L I N G L O G D A T A

LAYER NO.	DEPTH Z (IN.) FROM	TO	**** MATERIAL ****
1	0.0	0.7	SURFACE TREATMENT
2	0.7	6.7	LIMESTONE (RAW)
3	6.7	72.0	PLASTIC CLAY, MOIST
4	72.0	78.0	PLASTIC CLAY, DRY

SECTION 32 REPLICATION 1

U - DATA (MICRO-INCHES) FOR SINGLE 1000 LB. LOAD

DEPTH Z (IN.)	10.0	11.7	15.6	20.6	26.0	37.4	49.0	60.8	72.7	96.5	120.4	144.3	180.3	216.2
	**************	RADIAL	DISTANCE	R	(IN.)	**************								
0.0		-643	-290	-86	-150	-40	-14	20	30	18	15	12	NR	NR
1.5		-292	-235	-58	-68	18	15	30	22	18	12	NR	NR	NR
6.7		444	313	275	156	90	64	42	27	21	15	12	NR	NR
13.0		526	627	482	326	200	129	91	57	24	18	12	NR	NR
17.0		643	627	482	358	250	153	91	72	30	18	12	NR	NR
29.0		327	360	344	326	265	184	128	82	39	22	13	NR	NR
41.0		163	180	206	205	190	141	109	76	39	21	15	9	NR
53.0		70	86	103	110	112	92	70	48	30	18	12	NR	NR
65.0		26	27	41	45	50	49	36	33	23	16	12	NR	NR

DRILLING LOG DATA

LAYER NO.	DEPTH Z (IN.) FROM	TO	**** MATERIAL ****
1	0.0	0.7	SURFACE TREATMENT
2	0.7	6.7	LIMESTONE (RAW)
3	6.7	72.0	PLASTIC CLAY, MOIST
4	72.0	78.0	PLASTIC CLAY, DRY

SECTION 32 REPLICATION 2

W - DATA (MICRO-INCHES) FOR SINGLE 1000 LB. LOAD

DEPTH Z (IN.)	**************** R A D I A L						D I S T A N C E R				(I N .) ****************			
	10.0	11.7	15.6	20.6	26.0	37.4	49.0	60.8	72.7	96.5	120.4	144.3	180.3	216.2
0.0	2208	2085	1288	920	628	322	208	131	98	67	47	47	35	30
0.7	2812	2187	1437	1000	609	359	184	118	96	71	56	46	37	29
6.7	3000	2125	1375	906	656	343	175	121	99	74	57	48	39	31
13.0	2593	2000	1343	906	625	312	181	118	96	73	57	50	37	32
17.0	2125	1843	1312	875	656	343	196	128	99	71	56	48	37	31
29.0	937	875	765	546	437	271	162	112	93	74	51	43	35	28
41.0	656	671	609	546	453	318	224	153	118	81	62	50	39	32
53.0	375	393	359	343	318	262	209	140	112	87	65	51	37	34
65.0	287	250	243	253	218	218	181	125	109	81	59	46	31	28

D R I L L I N G L O G D A T A

LAYER NO.	DEPTH Z (IN.) FROM	TO	**** MATERIAL ****
1	0.0	0.7	SURFACE TREATMENT
2	0.7	8.0	LIMESTONE (RAW)
3	8.0	72.0	PLASTIC CLAY, MOIST

SECTION 32 REPLICATION 2

U - DATA (MICRO-INCHES) FOR SINGLE 1000 LB. LOAD

DEPTH Z (IN.)	************** RADIAL DISTANCE R (IN.) **************													
	10.0	11.7	15.6	20.6	26.0	37.4	49.0	60.8	72.7	96.5	120.4	144.3	180.3	216.2
0.0		-728	-296	-107	-142	-48	-19	22	34	21	17	14	10	9
0.7		-434	-267	-161	-108	-70	-21	17	11	11	10	10	8	8
4.0		182	91	43	19	15	15	14	17	13	10	11	8	10
6.7		354	199	90	60	33	33	24	23	13	9	8	8	8
8.0		577	298	154	114	45	39	28	28	14	10	10	8	7
13.0		474	375	265	197	109	87	53	44	19	14	11	8	8
17.0		468	386	322	254	177	117	81	51	34	22	13	11	9
29.0		212	270	268	242	187	125	83	57	24	13	8	6	5
41.0		148	149	159	159	141	111	72	59	30	17	10	9	7
53.0		69	76	87	91	90	69	56	42	23	15	10	8	6
65.0		22	27	31	35	38	36	31	26	16	12	9	8	7

D R I L L I N G L O G D A T A

LAYER NO.	DEPTH Z (IN.) FROM	TO	**** MATERIAL ****
1	0.0	0.7	SURFACE TREATMENT
2	0.7	8.0	LIMESTONE (RAW)
3	8.0	72.0	PLASTIC CLAY, MOIST